



Description of the atom-cavity system with a complex Hamiltonian

Babak Parvin

University of Maragheh, Maragheh, Iran

Abstract

In this study, we examine the behavior of a two-level atom confined within a single-mode optical cavity that is exposed to laser field radiation. Our analysis encompasses the consideration of the spontaneous emission of the two-level atom and its interaction with the cavity. The behavior of this system is explored through the application of Schrödinger's equation. The solutions to the equations describing the atom-cavity system have been calculated for both the general case and the weak driving limit. Comparative analysis of the numerical solutions with those obtained in the weak driving limit reveals a notable agreement.

Keywords: Optical cavity, Schrödinger equation, Two-level atom

AMS Mathematical Subject Classification [2010]: 81Q05, 81V80, 81P50

1 Introduction

A comprehensive analysis of a two-level atom confined within an optical cavity was conducted in [1]. This analysis utilized the master equation to describe the system's behavior, with solutions derived for both the general case and the weak driving limit. Subsequently, the numerical solution of the master equation was compared with results obtained under the weak driving limit.

In this work, we approach the model from the perspective of Schrödinger's equation. We provide solutions in both their full and approximate forms. Lastly, we compare our findings with those reported in [1].

2 Numerical solution

Within a single-mode optical cavity, a two-level atom is confined, and the cavity subjected to stimulation by a laser field. In this scenario, we describe the behavior of this system using the master equation as detailed in [1]:

$$\dot{\rho} = -i[H, \rho] + \kappa(2a\rho a^\dagger - a^\dagger a\rho - \rho a^\dagger a) + \gamma(2\sigma_- \rho \sigma_+ - \sigma_+ \sigma_- \rho - \rho \sigma_+ \sigma_-), \quad (1)$$

here, a and a^\dagger illustrate the cavity field's annihilation and creation operators, while σ_- and σ_+ denote the atomic lowering and raising operators. Additionally, κ signifies the decay rate of the cavity field, and γ

stands for the amplitude of the spontaneous emission rate. Now, let's proceed to define the Hamiltonian of this system in the interaction picture:

$$H = \delta_{AP}\sigma_+\sigma_- + \delta_{CP}a^\dagger a + g(a^\dagger\sigma_- + a\sigma_+) + Ea^\dagger + E^*a, \quad (2)$$

where $\delta_{AP} = \omega_A - \omega_P$ signifies the detuning between the atomic resonance and the probe laser, while $\delta_{CP} = \omega_C - \omega_P$ indicates the detuning between the cavity field and the probe laser. Additionally, we have the atom-cavity coupling constant denoted as g , and E , which is proportionate to the amplitude of the coherent-state probe laser at the optical frequency ω_P . Rather than using the master equation, we can describe this system using the following Hamiltonian [2–4]:

$$H_{eff} = (\delta_{AP} - i\gamma)\sigma_+\sigma_- + (\delta_{CP} - i\kappa)a^\dagger a + g(a^\dagger\sigma_- + a\sigma_+) + Ea^\dagger + E^*a, \quad (3)$$

in order to solve this formula, the Schrödinger equation can be utilized. To proceed, we write the wave function of the atom-cavity system as [5]:

$$|\psi\rangle = \sum_{n=0}^{\infty} c_{ng}|ng\rangle + c_{ne}|ne\rangle, \quad (4)$$

where $a^\dagger a|n\rangle = n|n\rangle$, $|g\rangle$, and $|e\rangle$ show the ground and excited levels of the atom, respectively. The parameters c_{ng} and c_{ne} indicate the expansion coefficients. We employ Schrödinger's equation, denoted as $H_{eff}|\psi\rangle = i|\dot{\psi}\rangle$, and by equating the corresponding coefficients on both sides, we arrive at the following result:

$$\dot{c}_{ng} = -(i\delta_{CP} + \kappa)nc_{ng} - iE\sqrt{n}c_{n-1g} - iE^*\sqrt{n+1}c_{n+1g} - ig\sqrt{n}c_{n-1e}, \quad (5)$$

$$\dot{c}_{ne} = -ig\sqrt{n+1}c_{n+1g} - (i\delta_{AP} + \gamma + (i\delta_{CP} + \kappa)n)c_{ne} - iE\sqrt{n}c_{n-1e} - iE^*\sqrt{n+1}c_{n+1e}, \quad (6)$$

furthermore, considering the wave function's normalization condition, we obtain the following equality:

$$\sum_{n=0}^{\infty} |c_{ng}|^2 + |c_{ne}|^2 = 1, \quad (7)$$

in order to illustrate these equations in a real form, one can establish the following relationships:

$$c_{ng} = x_n + iy_n, \quad (8)$$

$$c_{ne} = w_n + iz_n, \quad (9)$$

$$E = |E|e^{i\theta}, \quad (10)$$

after substituting these relationships into equations (5) through (7), we obtain:

$$\begin{aligned} \dot{x}_n = & \delta_{CP} n y_n - \kappa n x_n + |E| \cos\theta \sqrt{n} y_{n-1} + |E| \sin\theta \sqrt{n+1} x_{n-1} + |E| \cos\theta \sqrt{n+1} y_{n+1} - \\ & |E| \sin\theta \sqrt{n+1} x_{n+1} + g \sqrt{n} z_{n-1}, \end{aligned} \quad (11)$$

$$\begin{aligned} \dot{y}_n = & -\delta_{CP} n x_n - \kappa n y_n - |E| \cos\theta \sqrt{n} x_{n-1} + |E| \sin\theta \sqrt{n} y_{n-1} - |E| \cos\theta \sqrt{n+1} x_{n+1} - \\ & |E| \sin\theta \sqrt{n+1} y_{n+1} - g \sqrt{n} w_{n-1}, \end{aligned} \quad (12)$$

$$\begin{aligned} \dot{w}_n = & g \sqrt{n+1} y_{n+1} + (\delta_{AP} + \delta_{CP} n) z_n - (\gamma + \kappa n) w_n + |E| \cos\theta \sqrt{n} z_{n-1} + \\ & |E| \sin\theta \sqrt{n} w_{n-1} + |E| \cos\theta \sqrt{n+1} z_{n+1} - |E| \sin\theta \sqrt{n+1} w_{n+1}, \end{aligned} \quad (13)$$

$$\begin{aligned} \dot{z}_n = & -g \sqrt{n+1} x_{n+1} - (\delta_{AP} + \delta_{CP} n) w_n - (\gamma + \kappa n) z_n - |E| \cos\theta \sqrt{n} w_{n-1} + \\ & |E| \sin\theta \sqrt{n} z_{n-1} - |E| \cos\theta \sqrt{n+1} w_{n+1} - |E| \sin\theta \sqrt{n+1} z_{n+1}, \end{aligned} \quad (14)$$

$$\sum_{n=0}^{\infty} x_n^2 + y_n^2 + w_n^2 + z_n^2 = 1, \quad (15)$$

now, let's address these equations in the steady-state. To numerically solve them, we truncate the equations at a chosen value, denoted as N , and disregard the remaining equations. The choice of N should ensure that the solutions do not significantly change for $N - 1$ or $N + 1$. This simplifies the equations into the form $AV = B$, where A and B denote known matrices. By determining the V matrix, we resolve the problem, enabling us to calculate the desired physical quantities. Specifically, we aim to determine the behavior of the second-order correlation function at zero-time delay, which can be calculated using the following equation:

$$g^{(2)}(0) = \frac{\langle a^{\dagger 2} a^2 \rangle}{\langle a^{\dagger} a \rangle^2}, \quad (16)$$

where:

$$\langle a^{\dagger} a \rangle = \sum_{n=0}^{\infty} n(x_n^2 + y_n^2 + w_n^2 + z_n^2), \quad (17)$$

$$\langle a^{\dagger 2} a^2 \rangle = \sum_{n=0}^{\infty} (n^2 - n)(x_n^2 + y_n^2 + w_n^2 + z_n^2), \quad (18)$$

figure 1 displays the coherence function curve plotted with the following parameters: $g = 2\pi \times 34$ MHz, $\kappa = 2\pi \times 4.1$ MHz, $\gamma = 2\pi \times 2.6$ MHz, $|E| = 0.01\kappa$, and $\theta = 0$ as functions of δ_{CP} . Additionally, this curve assumes that $\delta_{AP} = \delta_{CP}$. When we extend this analysis to different values of θ , we observe that the curve's behavior remains consistent and aligns precisely with the blue dashed line. For the numerical solution, we employ $N = 50$ in the simulations. In the following section, we tackle these equations within the context of weak driving, ultimately deriving the explicit form of the second-order coherence function.

3 Explicit solution

In this section, we aim to compute the equations derived in the preceding section while considering the weak driving limit, where $|E| \ll \kappa$. Under these conditions, we indicate the order of the unknowns concerning $|E|$ as follows:

$$x_n \sim O(n), \quad y_n \sim O(n), \quad w_n \sim O(n+1), \quad z_n \sim O(n+1), \quad (19)$$

upon simplifying equations (11) through (15) to the second order of $|E|$, while retaining the dominant terms in each equation, we arrive at the following results:

$$\dot{x}_0 = 0, \quad (20)$$

$$\dot{y}_0 = 0, \quad (21)$$

$$\dot{w}_0 = gy_1 + \delta_{AP}z_0 - \gamma w_0, \quad (22)$$

$$\dot{z}_0 = -gx_1 - \delta_{AP}w_0 - \gamma z_0, \quad (23)$$

$$\dot{x}_1 = \delta_{CP}y_1 - \kappa x_1 + |E| \cos\theta y_0 + |E| \sin\theta x_0 + gz_0, \quad (24)$$

$$\dot{y}_1 = -\delta_{CP}x_1 - \kappa y_1 - |E| \cos\theta x_0 + |E| \sin\theta y_0 - gw_0, \quad (25)$$

$$\dot{w}_1 = g\sqrt{2}y_2 + (\delta_{AP} + \delta_{CP})z_1 - (\gamma + \kappa)w_1 + |E| \cos\theta z_0 + |E| \sin\theta w_0, \quad (26)$$

$$\dot{z}_1 = -g\sqrt{2}x_2 - (\delta_{AP} + \delta_{CP})w_1 - (\gamma + \kappa)z_1 - |E| \cos\theta w_0 + |E| \sin\theta z_0, \quad (27)$$

$$\dot{x}_2 = 2\delta_{CP}y_2 - 2\kappa x_2 + |E| \cos\theta \sqrt{2}y_1 + |E| \sin\theta \sqrt{2}x_1 + g\sqrt{2}z_1, \quad (28)$$

$$\dot{y}_2 = -2\delta_{CP}x_2 - 2\kappa y_2 - |E| \cos\theta \sqrt{2}x_1 + |E| \sin\theta \sqrt{2}y_1 - g\sqrt{2}w_1, \quad (29)$$

$$x_0^2 + y_0^2 = 1, \quad (30)$$

when these equations are solved in the steady-state, we can derive the following relationships:

$$c_{1g} = x_1 + iy_1 = \frac{-iE\tilde{\gamma}}{g^2 + \tilde{\kappa}\tilde{\gamma}} c_{0g} = a_1^{ss} c_{0g}, \quad (31)$$

$$c_{0e} = w_0 + iz_0 = \frac{-Eg}{g^2 + \tilde{\kappa}\tilde{\gamma}} c_{0g} = a_2^{ss} c_{0g}, \quad (32)$$

$$c_{2g} = x_2 + iy_2 = \frac{E^2(g^2 - \tilde{\gamma}(\tilde{\kappa} + \tilde{\gamma}))}{\sqrt{2}(g^2 + \tilde{\kappa}\tilde{\gamma})(g^2 + \tilde{\kappa}(\tilde{\kappa} + \tilde{\gamma}))} c_{0g} = a_3^{ss} c_{0g}, \quad (33)$$

$$c_{1e} = w_1 + iz_1 = \frac{iE^2g(\tilde{\kappa} + \tilde{\gamma})}{(g^2 + \tilde{\kappa}\tilde{\gamma})(g^2 + \tilde{\kappa}(\tilde{\kappa} + \tilde{\gamma}))} c_{0g} = a_4^{ss} c_{0g}, \quad (34)$$

here, we specify $\tilde{\kappa} = \kappa + i\delta_{CP}$ and $\tilde{\gamma} = \gamma + i\delta_{AP}$, and we use a_j^{ss} as defined in equation (3.6) from [1]. Assuming $c_{0g} = 1$, which corresponds to $x_0 = 1$ and $y_0 = 0$, we find that the solutions in equations (31) to (34) coincide with those given in equation (3.6) from [1]. The difference arises because [1] initially considers $c_{0g} = 1$, but in a general case, we can consider c_{0g} as a complex quantity in the form of $e^{i\phi}$, where ϕ is an arbitrary phase constant. Importantly, this phase constant has no impact on the ultimate physical solution of the problem. Now, let's proceed to calculate the second-order coherence function up to the dominant order as follows:

$$g^{(2)}(0) \simeq \frac{2(x_2^2 + y_2^2)}{(x_1^2 + y_1^2)^2} = \frac{2|c_{2g}|^2}{|c_{1g}|^4} = \frac{2|a_3^{ss}|^2}{|a_1^{ss}|^4 |c_{0g}|^2} = \frac{2|a_3^{ss}|^2}{|a_1^{ss}|^4}, \quad (35)$$

this corresponds precisely to the expression in equation (3.8) from [1]. The final equation is included due to the condition $|c_{0g}|^2 = 1$. Upon completing the calculations, the results are as follows:

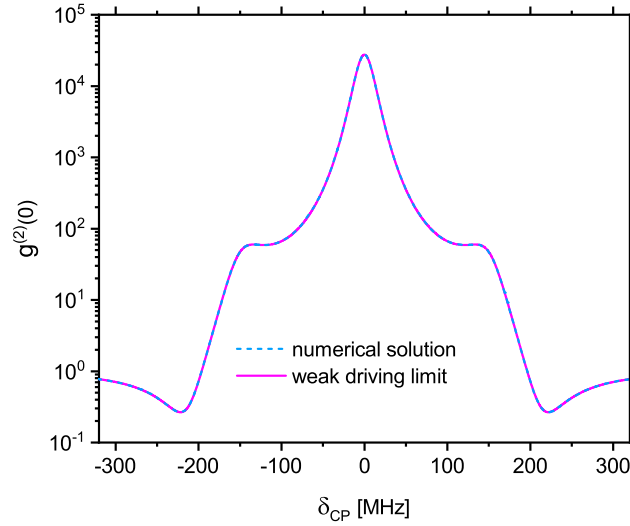


Figure 1: This figure illustrates the second-order coherence function curves for specified values versus probe laser detuning from the atomic resonance. The dashed curve corresponds to equation (16), while the solid curve corresponds to equation (36).

$$g^{(2)}(0) = \frac{s_1 s_2}{s_3^2 (x_0^2 + y_0^2) s_4} = \frac{s_1 s_2}{s_3^2 s_4}, \quad (36)$$

where the variables are outlined as:

$$s_1 = \delta_{AP}^2 \delta_{CP}^2 + \delta_{AP}^2 \kappa^2 - 2\delta_{AP} \delta_{CP} g^2 + \delta_{CP}^2 \gamma^2 + g^4 + 2g^2 \gamma \kappa + \gamma^2 \kappa^2, \quad (37)$$

$$s_2 = \delta_{AP}^4 + 2\delta_{AP}^3 \delta_{CP} + \delta_{AP}^2 \delta_{CP}^2 + 2\delta_{AP}^2 g^2 + 2\delta_{AP}^2 \gamma^2 + 2\delta_{AP}^2 \gamma \kappa + \delta_{AP}^2 \kappa^2 + 2\delta_{AP} \delta_{CP} g^2 + 2\delta_{AP} \delta_{CP} \gamma^2 + \delta_{CP}^2 \gamma^2 + g^4 - 2g^2 \gamma^2 - 2g^2 \gamma \kappa + \gamma^4 + 2\gamma^3 \kappa + \gamma^2 \kappa^2, \quad (38)$$

$$s_3 = \delta_{AP}^2 + \gamma^2, \quad (39)$$

$$s_4 = \delta_{AP}^2 \delta_{CP}^2 + \delta_{AP}^2 \kappa^2 + 2\delta_{AP} \delta_{CP}^3 - 2\delta_{AP} \delta_{CP} g^2 + 2\delta_{AP} \delta_{CP} \kappa^2 + \delta_{CP}^4 - 2\delta_{CP}^2 g^2 + \delta_{CP}^2 \gamma^2 + 2\delta_{CP}^2 \gamma \kappa + 2\delta_{CP}^2 \kappa^2 + g^4 + 2g^2 \gamma \kappa + 2g^2 \kappa^2 + \gamma^2 \kappa^2 + 2\gamma \kappa^3 + \kappa^4, \quad (40)$$

now, in figure 1, we can depict the curve corresponding to equation (36), derived under the weak field limit, illustrated as a solid pink line for given values in terms of δ_{CP} . The figure vividly demonstrates a remarkable agreement between the numerically generated results and the predictions within the weak driving limit. It's worth noting that this figure bears a striking resemblance to figure 3.1 featured in [1], which validates the accuracy of our calculations.

Conclusions

This work investigates the behavior of a two-level atom confined in a single-mode optical cavity in the steady-state. We have calculated the Schrödinger equation for this system in both the general case and the weak driving limit. The curves plotted based on these calculations demonstrate a consistent agreement

between the two methods. Regardless of whether we employ Schrödinger's equation or the master equation to describe the atom-cavity system's behavior, the outcomes remain consistent. Furthermore, these results remain unaffected by the θ phase of the probe laser.

References

- [1] A. Boca, *Experiments in cavity QED: Exploring the interaction of quantized light with a single trapped atom*, Thesis, California institute of technology, 2005.
- [2] H. J. Carmichael, *An open systems approach to quantum optics*, Lecture Notes in Physics, New Series: Monographs, Vol. 18, Springer, 1993.
- [3] F. Zou, X.-Y Zhang, X.-W Xu, J.-F. Haung, and J.-Q. Liao, *Multiphoton blockade in the two-photon Jaynes-Cummings model*, Phys. Rev. A 102 (2020) 053710.
- [4] J. P. Clemens, P. R. Rice, and L. M. Pedrotti, *Output spectrum of single-atom laser*, arXiv:quant-ph/9907085v2 (1999).
- [5] P. Hemphill, J. P. Clemens, *Intensity auto- and cross correlations for a three-level Λ -type atom in a driven, damped two-mode cavity*, J. Opt. Soc. Am. B 29 (2012) 1424-1429.

e-mail: `parvin@maragheh.ac.ir`